



Aalborg Universitet

AALBORG UNIVERSITY
DENMARK

Spared ulnar nerve injury results in increased layer III-VI excitability in the pig somatosensory cortex

Meijs, Suzan; Hayward, Andrew J; Gomes Nørgaard Dos Santos Nielsen, Thomas; Reidies Bjarkam, Carsten; Jensen, Winnie

Published in:
Lab Animal

DOI (link to publication from Publisher):
[10.1038/s41684-024-01440-0](https://doi.org/10.1038/s41684-024-01440-0)

Creative Commons License
CC BY 4.0

Publication date:
2024

Document Version
Publisher's PDF, also known as Version of record

[Link to publication from Aalborg University](#)

Citation for published version (APA):

Meijs, S., Hayward, A. J., Gomes Nørgaard Dos Santos Nielsen, T., Reidies Bjarkam, C., & Jensen, W. (2024). Spared ulnar nerve injury results in increased layer III-VI excitability in the pig somatosensory cortex. *Lab Animal*, 53(10), 287-293. <https://doi.org/10.1038/s41684-024-01440-0>

General rights

Copyright and moral rights for the publications made accessible in the public portal are retained by the authors and/or other copyright owners and it is a condition of accessing publications that users recognise and abide by the legal requirements associated with these rights.

- Users may download and print one copy of any publication from the public portal for the purpose of private study or research.
- You may not further distribute the material or use it for any profit-making activity or commercial gain
- You may freely distribute the URL identifying the publication in the public portal -

Take down policy

If you believe that this document breaches copyright please contact us at vbn@aub.aau.dk providing details, and we will remove access to the work immediately and investigate your claim.

<https://doi.org/10.1038/s41684-024-01440-0>

Spared ulnar nerve injury results in increased layer III–VI excitability in the pig somatosensory cortex

Check for updates

Suzan Meijs , Andrew J. Hayward¹, Thomas Gomes Nørgaard Dos Santos Nielsen ¹, Carsten Reidies Bjarkam^{2,3} & Winnie Jensen ¹

This study describes cortical recordings in a large animal nerve injury model. We investigated differences in primary somatosensory cortex (S1) hyperexcitability when stimulating injured and uninjured nerves and how different cortical layers contribute to S1 hyperexcitability after spared ulnar nerve injury. We used a multielectrode array to record single-neuron activity in the S1 of ten female Danish landrace pigs. Electrical stimulation of the injured and uninjured nerve evoked brain activity up to 3 h after injury. The peak amplitude and latency of early and late peristimulus time histogram responses were extracted for statistical analysis. Histological investigations determined the layer of the cortex in which each electrode contact was placed. Nerve injury increased the early peak amplitude compared with that of the control group. This difference was significant immediately after nerve injury when the uninjured nerve was stimulated, while it was delayed for the injured nerve. The amplitude of the early peak was increased in layers III–VI after nerve injury compared with the control. In layer III, S1 excitability was also increased compared with preinjury for the early peak. Furthermore, the late peak was significantly larger in layer III than in the other layers in the intervention and control group before and after injury. Thus, the most prominent increase in excitability occurred in layer III, which is responsible for the gain modulation of cortical output through layer V. Therefore, layer III neurons seem to have an important role in altered brain excitability after nerve injury.

Peripheral nerve injuries caused by trauma, surgery or disease (for example, diabetes) can evolve into persistent, severe and refractory neuropathic pain¹. Approximately 7–10% of the general population suffers from chronic neuropathic pain, and this is expected to increase due to the increased incidence of diabetes and increased survival after cancer therapy². Peripheral neuropathic pain involves damage to or inflammation of a peripheral nerve, which alters neuronal signaling and results in increased excitability of second-order spinal neurons^{3,4}, giving rise to allodynia and hyperalgesia⁵. Furthermore, patients with neuropathic pain often show signs of dysfunction in ascending and descending control pathways³. These peripheral and central changes contribute to altered signaling to the brain, which may result in cortical reorganization^{2,6}. Chronic pain can be difficult to treat, as even neuropathies with a clearly peripheral or central origin are influenced by a complex interplay of changes along the entire neuroaxis^{7,8}.

In rodents, numerous preclinical neuropathic models exist based on various etiologies of neuropathic pain⁹. These models allow invasive

investigations of mechanistic changes occurring after their induction. One such model is the spared nerve injury (SNI) model, which results in denervation in the area of the transected nerves and neuropathic pain in the area of the spared nerve¹⁰. This model has highlighted the contribution of noninjured neurons to the neuropathic pain pathology, including ectopic firing in injured and noninjured neurons and reinnervation of the denervated area by noninjured fibers¹¹. Hyperexcitability has also been shown in second-order superficial (lamina II)¹² and deep (lamina IV)¹³ dorsal horn spinal neurons after SNI⁴. Furthermore, SNI induces substantial brain alterations involving the descending modulatory pathways, the limbic system and the prefrontal and somatosensory cortices^{4,9,14–16}.

Studies in rodents have shown that activation of the primary somatosensory cortex (S1) increased immediately after SNI¹⁴, together with the information flow from S1 to the anterior cingulate cortex¹⁷. One day after SNI, S1 activation was decreased, and after 8 days, it was at a level comparable with that of sham animals¹⁴. This decrease in activation is thought to be related to the lack of input to the denervated S1 area^{14,17}.

¹Center for Neuroplasticity and Pain, Department of Health Science and Technology, Aalborg University, Aalborg, Denmark. ²Department of Clinical Medicine, Aalborg University, Aalborg, Denmark. ³Department of Neurosurgery, Aalborg University Hospital, Aalborg, Denmark. ✉e-mail: smeijs@hst.aau.dk

Although S1 activation was comparable between sham and SNI rats on day 8, a functional connection with the brainstem was only present in SNI rats, which is thought to be related to plasticity in the descending modulatory pathways¹⁴. With novel technologies, it has been possible to show robust hyperactivity in layer V of S1 in a mouse SNI model. This was caused by decreased activation of inhibitory interneurons in layer I and layer II/III, as well as increased inhibition of these interneurons^{4,18}.

Although rodents are the most well-developed models in pain research, it remains challenging to translate pharmaceutical results in these models to the clinic^{19,20}. For this reason, an increasing number of large animal pain models are being developed²¹. The pig's peripheral and central nervous system, body size and metabolism are comparable with those in humans^{22,23}. Furthermore, there is evidence that pigs with neuropathic injuries respond to pharmacological substances in a similar way as humans²⁴.

This study is an electrophysiological investigation of cortical excitability after nerve injury (NI) in the pig. The gyrated pig brain is much larger than the rodent brain²² and allows for independent intracortical recordings from different cortical layers. Therefore, the purpose of this study is twofold: to determine whether there was more S1 hyperactivity when stimulating the uninjured compared with the injured nerve and to investigate how different brain layers contribute to S1 hyperactivity. Central sensitization at the level of the spinal cord reaches its maximum within an hour after NI^{3,5,25}. We hypothesize that this would result in increased excitability in layer IV within the time frame of this study.

Results

Histological analysis was primarily used to determine the placement of the electrode contacts in the cortex. Analysis of seven pig brains showed an S1 cortical thickness of 2.4 ± 0.5 mm; low cellular density was found in layer I and higher cellular density in the deeper cortical layers. The neurons in layer I were the smallest ($5 \mu\text{m}$), while neurons in layer V were the largest ($15\text{--}20 \mu\text{m}$). No differences were observed between NI ($n = 4$) and control ($n = 3$) animals.

Spike sorting was performed to determine from how many neurons information was recorded and the characteristics of these neurons. Spikes were recorded from 1 to 3 units per channel, and most units were recorded from deeper layers, as most channels were placed in these. The evoked activity was never recorded from more than one neuron in layer I, while evoked activity was recorded from multiple units in layers II–VI (Table 1). The average spike amplitudes appeared larger in layers I and II compared with layers III–VI (Fig. 1a). Spike waveforms from a representative experiment are shown in Fig. 1b. Spontaneous firing was observed between stimulations, and corresponding firing rates were generally low (<10 spikes per second), with occasional bursts of activity displaying higher firing rates (mostly below 300 spikes per second) that often occurred in layers III and IV (Fig. 1c). Evoked firing rates consistently reached up to 740 spikes per second in every layer.

Brain excitability is increased after NI when the injured and uninjured nerves are stimulated

Spikes were binned into 1 ms bins to obtain peristimulus time histograms (PSTHs). Repeated measure analysis of variance (RM-ANOVA) was performed on the average PSTH of each pig upon stimulation of the (injured) ulnar and (uninjured) median nerve. An early and a late peak were consistently observed in the PSTHs, and the amplitude and latency of these peaks were analyzed separately. There was a significant two-way interaction between time and intervention for the early peak amplitude ($F(6,42) = 2.942$; $P = 0.017$; observed power of 0.85, RM-ANOVA). There was no significant effect of stimulating the injured or uninjured nerve (Fig. 2a). There were also no statistically significant differences between intervention and control groups at baseline ($P = 0.12$, RM-ANOVA). However, post hoc pairwise comparisons revealed that for the ulnar nerve, the early peak of the NI group ($n = 6$) was significantly greater than that of

Table 1 | The number of channels in each layer for the NI and control group

Layer	NI ($n = 4$)		Control ($n = 3$)		Total ($n = 7$)
	Channels	Neurons	Channels	Neurons	Total neurons
I	2	2	4	4	6
II	3	6	1	2	8
III	7	11	7	9	20
IV	10	13	8	12	25
V	33	38	13	20	58
VI	8	10	5	6	16
Total	63	80	38	53	133

the control group ($n = 3$), only in the last three phases after NI ($P < 0.05$; confidence interval (CI) 224 to 1,737 at 180 min) (Fig. 2b), while the difference between the two groups was significant for every phase after NI ($P < 0.05$; CI 717 to 1,787 at 180 min) when the median nerve was stimulated (Fig. 2c). The same interaction was found in the statistical analysis for the normalized data shown in Fig. 2d,e ($F(6,42) = 3.331$; $P = 0.009$; observed power of 0.90, RM-ANOVA).

Residuals were normally distributed for peak latency in both time windows and for peak amplitude in the 10–19 ms time window, but not in the 21–35 ms time window. It was chosen not to study the second peak further in the RM-ANOVA analysis, and the results presented in Fig. 2 are, therefore, based solely on the early peak. There were no significant effects or interactions for peak latencies in the early time window. The mean latency (center of mass, CoM) of the first and the second peak in the median nerve was 14.9 ± 0.2 ms and 26.4 ± 0.7 ms, respectively, and in the ulnar nerve 14.6 ± 0.3 ms and 25.9 ± 0.6 ms, respectively. The latency of the early peak was consistent with the nerve fiber conduction velocity of 66 ± 8 m/s and 60 ± 8 m/s, which corresponds to A β fiber activation. A secondary fiber group with a conduction velocity of 26 m/s could be distinguished in some of the recordings, which corresponds to A δ fiber activation.

Late-evoked peak is the largest in layer III

ANOVA analysis showed that the responses evoked by stimulation of the injured and uninjured nerves were not significantly different from each other. These were, therefore, grouped in the mixed model analysis, which investigated the differences between cortical layers and the effect of SNI on each of the layers. The significant parameters of each of the models are listed in Table 2. Post hoc pairwise comparisons revealed that the amplitude of the second peak (21–35 ms after the stimulus) was significantly larger in layer III (32.1 ± 8.4 spikes/bin) compared with all other layers ($P \leq 0.005$; CI largest difference (layer III–I) 10.5 to 28.1; CI smallest difference (layer III–IV) 5 to 16). This difference was consistent throughout the duration of the experiment but most notable in control and intervention groups before intervention (Fig. 3). Furthermore, the amplitude of the second peak was significantly larger in layer IV compared with layers I and VI, which was only significant before intervention ($P < 0.001$, mixed model pairwise comparisons; CI (layer IV–I) 0.4 to 17.4; CI (layer IV–VI) 0.9 to 12.0). For both peaks, the amplitude was significantly smaller in layer I compared with layers III–VI before intervention ($P \leq 0.003$, mixed model pairwise comparisons; late peak layer I versus VI: $P = 0.03$, mixed model pairwise comparisons, CI -0.6 to 29.6) but not in the phases after NI and control. The amplitude of the first peak (10–19 ms after the stimulus) showed no statistically significant differences across layers. Post hoc comparisons revealed no significant differences between layers in peak latency.

SNI results in increased evoked activity in layer III compared with the control and preinjury

The mixed model pairwise comparisons only showed significant differences between the control and NI group (main effects) for the amplitude

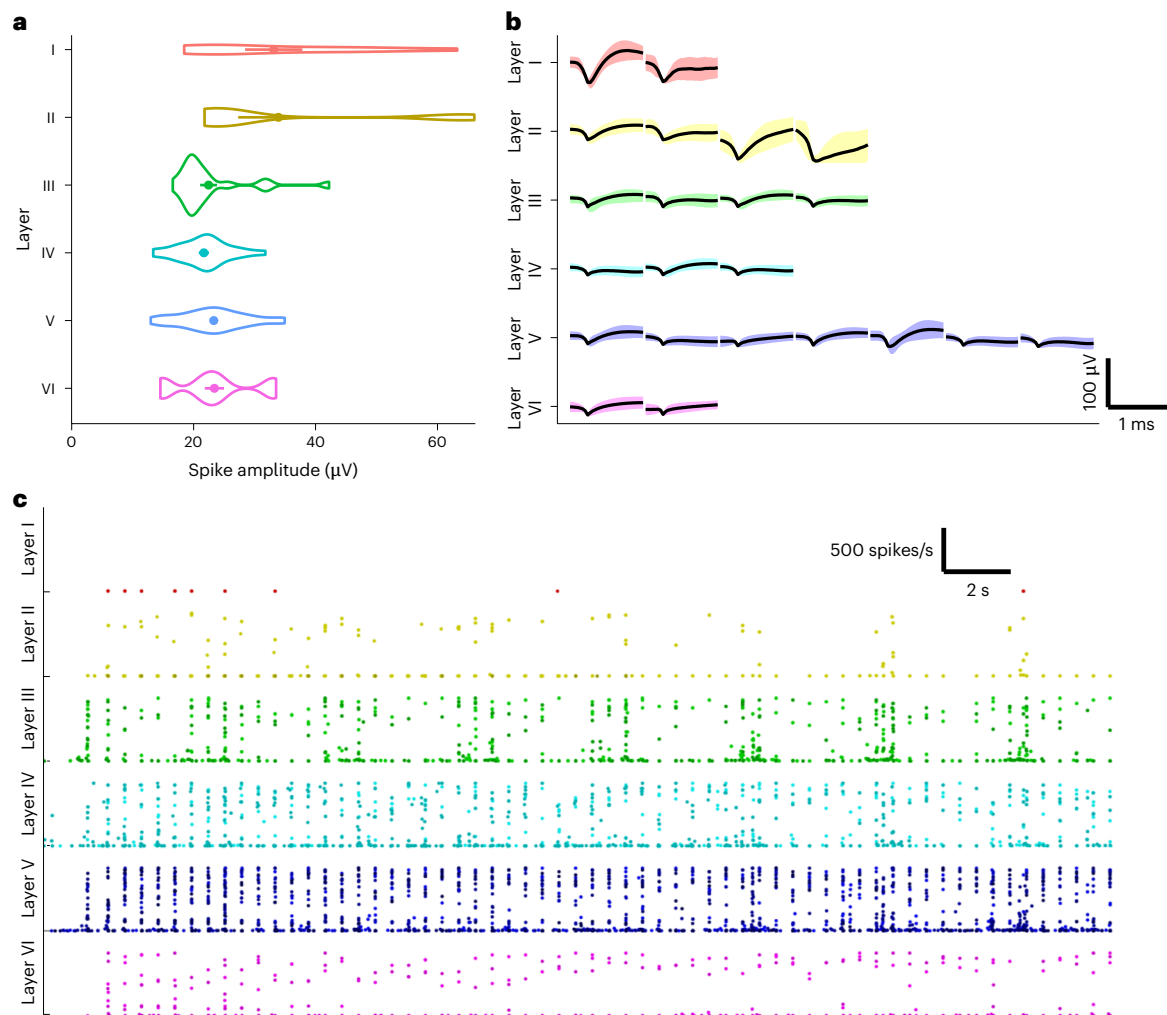


Fig. 1 | Characteristics of spikes recorded from S1 cortical layers I–VI. a, The average spike amplitudes in different layers of the pig cortex across all experiments. **b,** The spike waveforms recorded from different layers of the pig cortex from a representative experiment. Since layer V is relatively thick, most channels were placed in this layer, and most neurons were recorded here as well. **c,** The firing patterns in different layers of the cortex from the same experiment; different shades of the same color represent different units. The timeline starts 2 s before stimulation. Layer I had a small response to stimulation, and these channels were excluded from the analysis. Layer II was more responsive, with sometimes several spikes per stimulus. Other experiments showed more activity in layer II, yet it was

never as tightly correlated with the stimulus timing as observed in layers III–VI. In layers III–VI, consistent firing can be observed after every stimulus (striped pattern). In layers III and IV, periods of higher and lower evoked activity can be distinguished at 4 s intervals. These periods of high activity also correspond to increased firing in layer II, where such bands of activity were also observed later in the experiment and in other experiments. In layers V and VI, firing patterns showed a reliable correlation to the stimulus and bands of increased activity were not observed. The length of the scale bars (in **b** and **c**) depicts the time and amplitude axes.

of the early peak (10–19 ms after stimulus). Figure 3 visualizes the development of both the early and late peak throughout the experiment in the NI and control group. Figure 4 shows that the early peak in layer III was significantly larger in the NI group than in the control group at all times after NI ($P < 0.03$, mixed model pairwise comparisons; CI at 60 min 23.6 to 120.3). This was also the case in layers IV and V at all times, except 90 min after NI ($P \leq 0.04$, mixed model pairwise comparisons; CI layer IV at 60 min 11.3 to 105.9; CI layer V at 60 min 4.2 to 95.6) and in layer VI at all times, except 90 and 120 min after NI ($P < 0.03$, mixed model pairwise comparisons; CI layer VI at 60 min 9.6 to 106.5).

In line with these findings, significant main effects were found for the NI group within layer III ($F(6,63) = 4.029$, $P = 0.002$), where the amplitude of the early peak was significantly greater at all times after NI compared with before (150 min: $P = 0.03$; all other phases: $P \leq 0.01$, mixed model pairwise comparison; CI at 60 min 8.8 to 64.7). This effect was not seen in the control group or in other cortical layers. Additionally, the peak amplitude of the early and late peaks in layer I within the control

group was significantly lower before intervention compared with after (early peak: 90–180 min, late peak: 120–180 min).

Discussion

In this study, we investigate how the injured and uninjured nerves contribute to S1 hyperactivity and how different cortical layers contribute to increased S1 excitability in the first hours after NI. The amplitude of the first peak significantly increased after NI compared with the control when the injured and uninjured nerves were stimulated. The increased amplitude was only observed in the deeper layers of the cortex (layers III–VI) and was most prominent in layer III.

Increased excitability after NI compared with the control

A significant increase in excitability was observed in the NI group compared with the control for both the (uninjured) median and (injured) ulnar nerve. This increase is significantly different from the control group immediately after SNI for the median nerve and 120 min after SNI for the

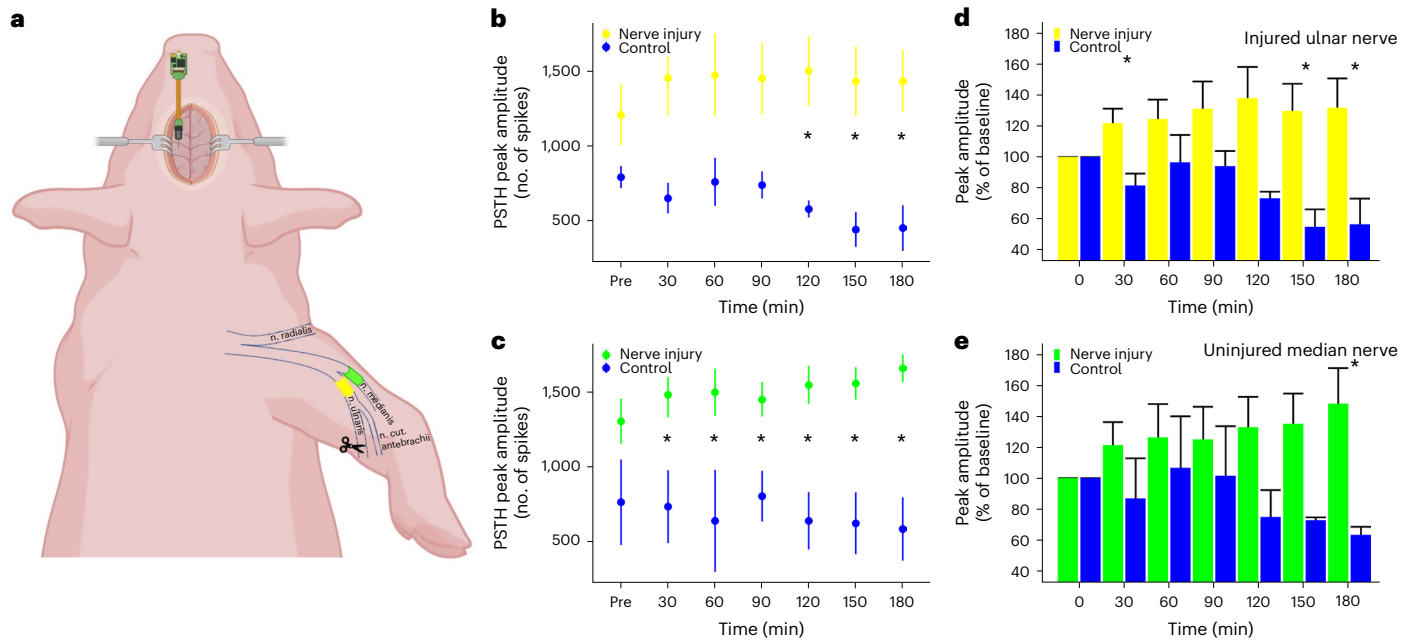


Fig. 2 | The early peak responses evoked by median and ulnar nerve stimulation are significantly increased compared with the control. **a**, Stimulation was applied to the ulnar and median nerves before and after the ulnar nerve was injured distal to the stimulation site. The cortical signals were recorded using a penetrating electrode in S1. The figure was created with [BioRender.com](https://www.biorender.com). **b**, The peak amplitude of the early cortical response to stimulation of the ulnar nerve was significantly higher in the NI group ($n = 6$) compared with the control group ($n = 3$) from 2 h after the injury. **c**, When the median nerve was stimulated, the early cortical

response was significantly higher in the NI group compared with the control group at every time point after injury of the ulnar nerve. The results are presented as estimated marginal means, and the error bars indicate the standard error of the mean. **d,e**, The peak amplitudes in the NI groups increase up to 140% and 150% compared with the baseline for the ulnar (**d**) and median nerves (**e**), respectively. The peak amplitude in the control group drops in the last 90 min of the experiment. * $P < 0.05$, RM-ANOVA. n. cut. antibrachii, antibrachial cutaneous nerves.

Table 2 | Significant mixed model parameters for each of the independent variables

Dependent variable	Significant factors	F	P
Early peak amplitude	Layer	$F(5,105) = 2.751$	0.022
	Intervention	$F(1,7) = 5.704$	0.048
	Layer \times phase	$F(36,199) = 2.859$	<0.001
	Layer \times intervention \times phase	$F(37,189) = 2.029$	0.001
Late peak amplitude	Layer	$F(5,114) = 8.152$	<0.001
	Layer \times phase	$F(36,148) = 3.740$	<0.001
	Layer \times intervention \times phase	$F(38,94) = 3.152$	<0.001
Early CoM	Phase	$F(6,47) = 2.326$	0.048
	Layer \times phase	$F(35,268) = 5.805$	<0.001
	Layer \times intervention \times phase	$F(38,94) = 4.314$	<0.001
Late CoM	Phase	$F(6,77) = 2.474$	0.030
	Layer \times phase	$F(35,334) = 2.004$	0.001
	Phase \times intervention	$F(7,22) = 2.625$	0.039

ulnar nerve. This is in line with Tøttrup et al., who found a delayed increase in the evoked S1 responses after SNI upon nonnociceptive stimulation of the injured nerve. For higher stimulation intensities, they observed a similar trend, where the greatest difference was observed between the latest recording and baseline²⁶.

The (not significant) difference between the injured and uninjured nerves could be due to the partial denervation, which compromises activation of the injured fibers and thereby provides less input to the brain. Alternatively, an increase in evoked activity could be masked by a tonic increase in background activity¹⁴. Such sensitization of S1 was observed

by Chao et al., who reported tonically increased nonevoked activity in S1 of rats in the first minutes after SNI¹⁴.

Increased excitability in deeper cortical layers (III–VI)

This study showed a significantly increased cortical activation after NI compared with the control in layers III–VI but not in layers I and II. While responses for the NI group were constant in layers I and II, the contacts in layer I of the control group were unreliable, most probably due to poor tissue contact at the start of the experiment. Our results resemble the increased activity in layer V and decreased activity of inhibitory interneurons in layer I found in mice at rest 1 week and 1 month after SNI¹⁸. The same authors found both an increase in vasoactive intestinal polypeptide-positive cells and a decrease in somatostatin- and parvalbumin-expressing cells in layer II/III¹⁸. In rodents, laminar dissociation is not always clear²⁷. However, here, layer II and layer III could be investigated separately due to the larger size of the pig brain and a clearer distinction between layers²⁸. While no significant increase in activity was seen in layer II, the largest increase in activity was seen in layer III, which indicates distinct physiology between these layers. We speculate that the lack of change in activity in layer II may be due to the aforementioned combination of an increase in inhibition and a decrease in the activity of inhibitory interneurons. Based on the recorded firing patterns, fast-spiking interneurons dominate the results; however, methods used in this study cannot discriminate between inhibitory or excitatory function of these interneurons.

Peripheral stimulation of the median and ulnar nerve evoked two peaks of activity in the pig S1 with latencies of 15 and 26 ms. These latencies correspond to conduction velocities of A β (60 and 66 m/s) and A δ (26 m/s) fiber populations. These conduction velocities are consistent with the stimulation intensity and nerve fiber activation pattern of the ulnar nerve in pigs²⁹. Increased excitability was primarily found for the early peak. This increase could, therefore, be a cortical expression of allodynia,

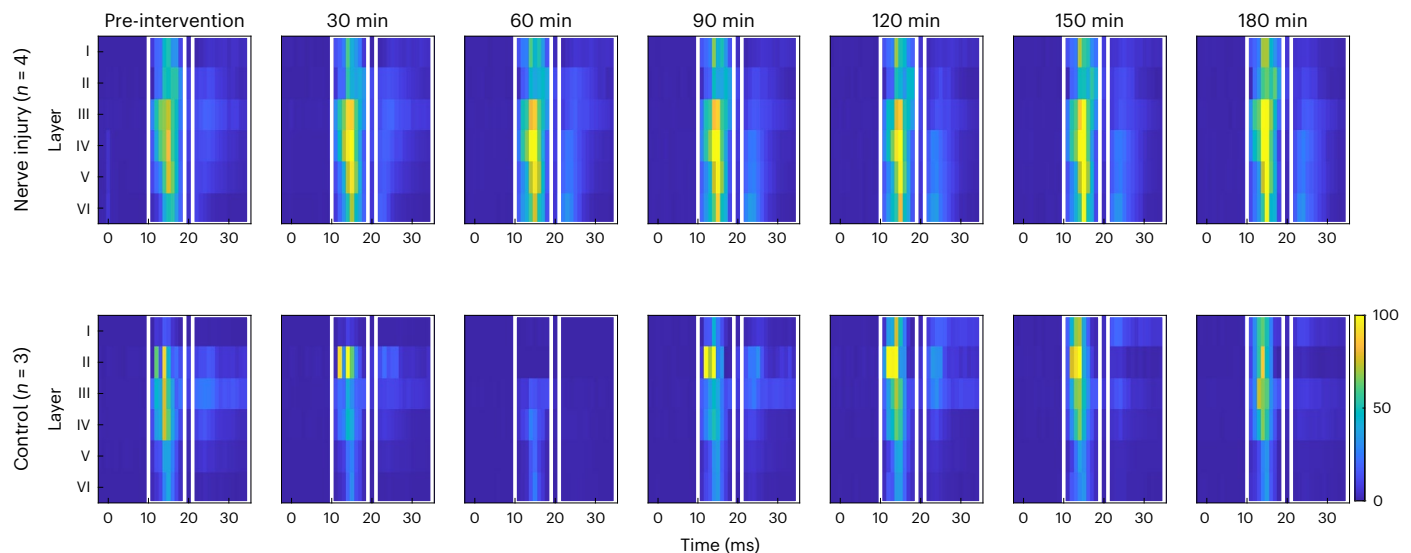


Fig. 3 | PSTHs recorded from the layers I–VI of the pig cortex. The increased excitability in deeper layers (III–VI) of the cortex after NI can be discerned (note that the number of spikes is capped at 100 spikes per bin), while superficial layers (I and II) seem to have a more constant response to electrical stimulation of the median and ulnar nerves. In the control group, the stimulus-evoked activity

seems constant and concentrated in layers I–IV (apart from missing data from one animal at 60 min and possibly poor contact in layer I at the beginning of the experiments). The white boxes indicate the early and late cortical responses to stimulation. The color axis denotes the number of spikes per bin, which is capped at 100 spikes to allow visualization of the second peak.

which has been found in other NI studies in pigs^{24,30,31}. In rodents, it has been demonstrated that allodynia occurs in the areas innervated by the injured as well as uninjured nerves¹⁰, which is consistent with our findings. The second peak corresponds to A δ fiber activation and was significantly larger in layer III compared with all other layers, both before and after intervention and in both groups. Interestingly, layers II/III are known for their gain-control function within the laminar circuitry, in particular to layer V, which projects to subcortical structures (for example, thalamus and brainstem)³². Layer III neurons are known to be sensitive to modulation by contextual information and arousal level³². Therefore, the increased late peak in this layer may be of particular significance for pain processing.

Increased cortical excitability in layer III after NI compared with the baseline

Interestingly, we observed the greatest increase in cortical excitability after NI compared with the baseline in layer III (46% compared with 20% in layer IV), which might indicate cortical sensitization between layer IV and layer III neurons. Again, this finding points toward a specific role of layer III in pain processing. In line with previous studies^{18,32}, increased activity in layer III may drive the increased excitability in layers V and VI, as layer III contains feedforward neurons projecting to layer V (ref. 27).

An alternative theory could be suggested based on the direct pathway proposed by Constantinople and Bruno³³. According to the conventional indirect pathway, signals arrive at layer IV, are projected to layer III and, from there, are further conveyed to layers V and VI. Constantinople and Bruno³³ proposed the direct pathway after the thalamus, which was found to project directly to layers V and VI, even when layer IV was inactivated by lidocaine. This manipulation removed both input to as well as signal transmission through layer IV, yet activity in layers V and VI remained almost unchanged³³. According to the direct theory, the similar increase in excitability that was observed in layers IV, V and VI (14–20% increase after NI compared with the baseline) could be expected, if this is indeed driven by spinal hyperactivity^{4,13}. The deeper cortical layers, also project back to the thalamus and brainstem, where alterations in descending modulation may occur¹⁴.

We found no statistically significant differences between the latencies of the responses in the different layers ($P=0.092$ and $P=0.051$, mixed model for the early and late peaks, respectively). This finding would

be in line with the direct thalamocortical pathway theory for the deep cortical layers (layer IV–VI). However, a delay was expected for layers II/III (ref. 33).

Limitations

This is one of the first studies developing a translational model of pain in pigs with recording of brain signals^{21,34}. So far, there are no chronic pain studies in pigs that recorded brain signals²¹. Likewise, we started our translational work with acute studies. Therefore, we do not yet know what pain phenotype the pig will develop after the transection of the ulnar nerve. The invasiveness of the brain recordings performed in this study does not allow for the animals to survive. Nevertheless, other nerve damage models have been used in behavioral studies in the pig, including nerve crush³¹, peripheral neuritis trauma^{24,31,35} and nerve transection models³⁰. These studies show that pigs develop allodynia, mechanical hyperalgesia^{24,30,31} and motor deficits depending on the injury^{30,31}. Future research should combine less invasive chronic electrophysiological recordings with behavioral assessment after NI in the forelimb.

Our methodology does not provide information about the function of the neurons that we have recorded. It is, thus, difficult to determine the consequences of the hyperexcitability reported here. Immunohistochemistry, pharmacological or optogenetic methods may provide means to further investigate the functions of cortical neurons in the pig. Since the pig model is relatively novel in pain research²¹, these methods are not yet developed. It is, however, possible to stain somatostatin-, vasoactive intestinal polypeptide- and parvalbumin-expressing cells in the pig brain^{36,37}, and future research should investigate in which layers of the cortex these neurons are predominant.

A nonsignificant decrease in the peak amplitudes was observed in the control group 2 h after the sham intervention. Anesthetics were kept as low as ethically acceptable to facilitate good quality evoked responses³⁸. However, a buildup effect is likely to have influenced the recordings during the last 2 h of the experiment. Since this is expected to have the same effect on both groups, the difference between them indicates that NI indeed led to hyperexcitability compared with a sham intervention.

Furthermore, few channels were placed in layers I and II, which were relatively thin and layer I was sparse in neuronal density in line with previous studies^{28,39}. This led to the exclusion of three unresponsive

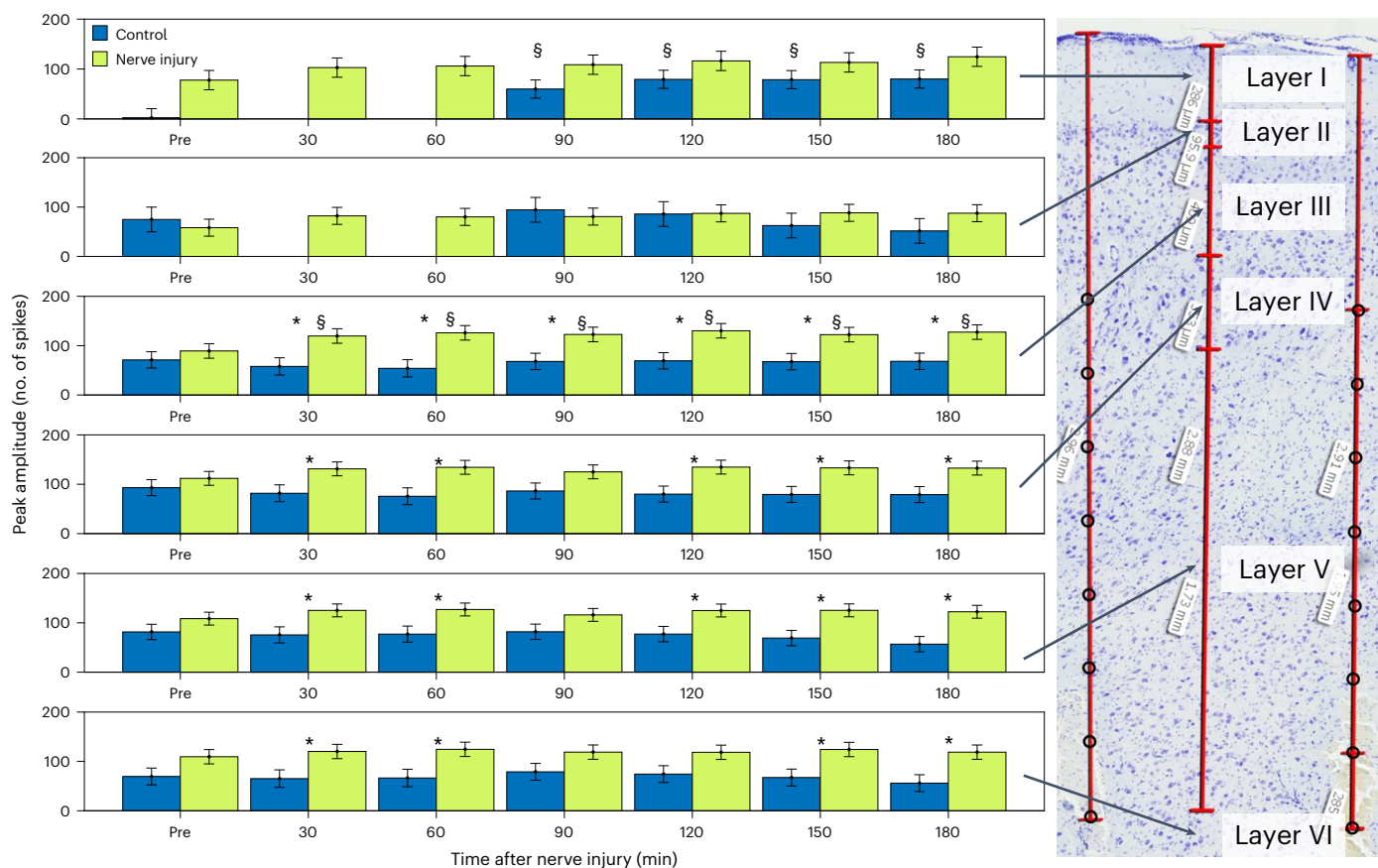


Fig. 4 | The early peak amplitude is significantly increased in layers III–VI of S1, with layer III showing the largest significant increase compared with the baseline and control. The peak amplitude of the PSTH (mean number of spikes per channel) was significantly increased in deeper layers of the cortex after NI compared with the control. In layer III, excitability was also increased after injury in the NI group compared with the baseline. In layer I, there was a lack of activity

at baseline in the control group, and data are missing for this same group in the first two stimulation series after intervention. The sample sizes are the number of channels placed in each layer presented in Table 1. The results are presented as estimated marginal means, and the error bars indicate the standard error of the mean. * $P < 0.05$ compared with the control. § $P < 0.05$ compared with the baseline, mixed model pairwise comparisons.

channels in layer I of one control and one intervention animal. Although we have independent recordings in these layers, this constraint makes it difficult to conclude on the results from them. The peak amplitudes were significantly smaller in layer I compared with all other layers. This is probably due to poor electrode–cell contact in layer I at the start of the experiment, as it was only found before intervention in the control group.

Impact

Significant increased excitability in S1 layers III–VI occurred during a timescale of 3 h. These findings are in line with results from rodent SNI models and warrant longer term studies to unravel whether these changes persist and influence behavior. Changes in layers V and VI could have an influence on descending controls¹⁴, which has been observed in patients. This study further adds to the evidence pointing to the need to take central nervous system changes into account when developing novel treatments for peripheral neuropathic pain⁷.

Conclusions

This study shows increased porcine cortical responses immediately after NI compared with the control when the uninjured median nerve is stimulated. This difference is also significant from 2 h after intervention, when the injured ulnar nerve is stimulated. We further show that hyperexcitability occurs in deeper cortical layers (III–VI), which could indicate an ascending mechanism. The increase in excitability was significant and most prominent compared with the baseline in layer III, which modulates

excitability in cortical output layer V. Furthermore, the amplitude of the late peak was greater in layer III than all other layers, which indicates that this layer may have a significant role in pain processing.

Online content

Any methods, additional references, Nature Portfolio reporting summaries, source data, extended data, supplementary information, acknowledgements, peer review information; details of author contributions and competing interests; and statements of data and code availability are available at <https://doi.org/10.1038/s41684-024-01440-0>.

Received: 13 July 2023; Accepted: 21 August 2024

Published online: 30 September 2024

References

1. Campbell, J. N. & Meyer, R. A. Mechanisms of neuropathic pain. *Neuron* **52**, 77–92 (2006).
2. Colloca, L. et al. Neuropathic pain. *Nat. Rev. Dis. Primers* **3**, 17002 (2017).
3. Sandkühler, J. & Liu, X. Induction of long-term potentiation at spinal synapses by noxious stimulation or nerve injury: LTP in spinal cord induced by noxious stimulation. *Eur. J. Neurosci.* **10**, 2476–2480 (1998).
4. Guida, F. et al. Behavioral, biochemical and electrophysiological changes in spared nerve injury model of neuropathic pain. *IJMS* **21**, 3396 (2020).

5. Ruscheweyh, R., Wilder-Smith, O., Drdla, R., Liu, X.-G. & Sandkühler, J. Long-term potentiation in spinal nociceptive pathways as a novel target for pain therapy. *Mol. Pain* **7**, 20 (2011).
6. Andoh, J., Milde, C., Tsao, J. W. & Flor, H. Cortical plasticity as a basis of phantom limb pain: fact or fiction? *Neuroscience* **387**, 85–91 (2018).
7. Hung, P. S.-P., Chen, D. Q., Davis, K. D., Zhong, J. & Hodaie, M. Predicting pain relief: use of pre-surgical trigeminal nerve diffusion metrics in trigeminal neuralgia. *NeuroImage Clin.* **15**, 710–718 (2017).
8. Haroutounian, S. et al. How central is central poststroke pain? The role of afferent input in poststroke neuropathic pain: a prospective, open-label pilot study. *Pain* **159**, 1317–1324 (2018).
9. Jaggi, A. S., Jain, V. & Singh, N. Animal models of neuropathic pain: animal models of neuropathic pain. *Fundam. Clin. Pharmacol.* **25**, 1–28 (2011).
10. Decosterd, I. & Woolf, C. J. Spared nerve injury: an animal model of persistent peripheral neuropathic pain. *Pain* **87**, 149–158 (2000).
11. Chen, W. et al. Accumulation of Cav3.2 T-type calcium channels in the uninjured sural nerve contributes to neuropathic pain in rats with spared nerve injury. *Front. Mol. Neurosci.* **11**, 24 (2018).
12. Guida, F. et al. PC1, a non-peptide PKR1-preferring antagonist, reduces pain behavior and spinal neuronal sensitization in neuropathic mice. *Pharmacol. Res.* **91**, 36–46 (2015).
13. Ding, L., Cai, J., Guo, X.-Y., Meng, X.-L. & Xing, G.-G. The antiallodynic action of pregabalin may depend on the suppression of spinal neuronal hyperexcitability in rats with spared nerve injury. *Pain Res. Manag.* **19**, 205–211 (2014).
14. Chao, T.-H. H., Chen, J.-H. & Yen, C.-T. Plasticity changes in forebrain activity and functional connectivity during neuropathic pain development in rats with sciatic spared nerve injury. *Mol. Brain* **11**, 55 (2018).
15. Cardoso-Cruz, H., Lima, D. & Galhardo, V. Impaired spatial memory performance in a rat model of neuropathic pain is associated with reduced hippocampus-prefrontal cortex connectivity. *J. Neurosci.* **33**, 2465–2480 (2013).
16. Palazzo, E. et al. EPI receptor within the ventrolateral periaqueductal grey controls thermonociception and rostral ventromedial medulla cell activity in healthy and neuropathic rat. *Mol. Pain* **7**, 82 (2011).
17. Tøttrup, L., Atashzar, S. F., Farina, D., Kamavuako, E. N. & Jensen, W. Altered evoked low-frequency connectivity from SI to ACC following nerve injury in rats. *J. Neural Eng.* **18**, 046063 (2021).
18. Cichon, J., Blanck, T. J. J., Gan, W.-B. & Yang, G. Activation of cortical somatostatin interneurons prevents the development of neuropathic pain. *Nat. Neurosci.* **20**, 1122–1132 (2017).
19. Percie du Sert, N. & Rice, A. S. C. Improving the translation of analgesic drugs to the clinic: animal models of neuropathic pain: Improving models of neuropathic pain. *Br. J. Pharmacol.* **171**, 2951–2963 (2014).
20. Henze, D. A. & Urban, M. O. in *Translational Pain Research: From Mouse to Man* (eds Kruger, L. & Light, A. R.) (CRC Press, 2009).
21. Meijis, S., Schmelz, M., Meilin, S. & Jensen, W. A systematic review of porcine models in translational pain research. *Lab Anim.* **50**, 313–326 (2021).
22. Sauleau, P., Lapouble, E., Val-Laillet, D. & Malbert, C.-H. The pig model in brain imaging and neurosurgery. *Animal* **3**, 1138–1151 (2009).
23. Cobianchi, L. et al. Pain assessment in animal models: do we need further studies? *JPR* <https://doi.org/10.2147/JPR.S59161> (2014).
24. Castel, D., Sabbag, I., Brenner, O. & Meilin, S. Peripheral neuritis trauma in pigs: a neuropathic pain model. *J. Pain* **17**, 36–49 (2016).
25. Zhang, H.-M. et al. Acute nerve injury induces long-term potentiation of C-fiber evoked field potentials in spinal dorsal horn of intact rat. *Sheng Li Xue Bao* **56**, 591–596 (2004).
26. Tøttrup, L., Diaz-Valencia, G., Kamavuako, E. N. & Jensen, W. Modulation of SI and ACC response to noxious and non-noxious electrical stimuli after the spared nerve injury model of neuropathic pain. *Eur. J. Pain* **25**, 612–623 (2021).
27. Rockland, K. S. What do we know about laminar connectivity? *NeuroImage* **197**, 772–784 (2019).
28. Bjarkam, C. R., Glud, A. N., Orłowski, D., Sørensen, J. C. H. & Palomero-Gallagher, N. The telencephalon of the Göttingen minipig, cytoarchitecture and cortical surface anatomy. *Brain Struct. Funct.* **222**, 2093–2114 (2017).
29. Andreis, F. R. et al. The use of the velocity selective recording technique to reveal the excitation properties of the ulnar nerve in pigs. *Sensors* **22**, 58 (2021).
30. Hellman, A. et al. Development of a common peroneal nerve injury model in domestic swine for the study of translational neuropathic pain treatments. *J. Neurosurg.* **135**, 1–8 (2021).
31. Rice, F. L. et al. Human-like cutaneous neuropathologies associated with a porcine model of peripheral neuritis: a translational platform for neuropathic pain. *Neurobiol. Pain* **5**, 100021 (2019).
32. Quiquempoix, M. et al. Layer 2/3 pyramidal neurons control the gain of cortical output. *Cell Rep.* **24**, 2799–2807.e4 (2018).
33. Constantinople, C. M. & Bruno, R. M. Deep cortical layers are activated directly by thalamus. *Science* **340**, 1591–1594 (2013).
34. Janjua, T. A. M. et al. The effect of peripheral high-frequency electrical stimulation on the primary somatosensory cortex in pigs. *IBRO Neurosci. Rep.* **11**, 112–118 (2021).
35. Castel, D., Sabbag, I., Nasaev, E., Peng, S. & Meilin, S. Open field and a behavior score in PNT model for neuropathic pain in pigs. *JPR* **11**, 2279–2293 (2018).
36. Ettrup, K. S., Sørensen, J. C. & Bjarkam, C. R. The anatomy of the Göttingen minipig hypothalamus. *J. Chem. Neuroanat.* **39**, 151–165 (2010).
37. Równiak, M. et al. Somatostatin-like immunoreactivity in the amygdala of the pig. *Folia Histochem. Cytobiol.* **46**, 229–238 (2008).
38. Kortelainen, J. et al. in *2014 36th Annual International Conference of the IEEE Engineering in Medicine and Biology Society* 4286–4289 (IEEE, 2014).
39. Muralidhar, S., Wang, Y. & Markram, H. Synaptic and cellular organization of layer 1 of the developing rat somatosensory cortex. *Front. Neuroanat.* **7**, 52 (2014).

Publisher's note Springer Nature remains neutral with regard to jurisdictional claims in published maps and institutional affiliations.

Open Access This article is licensed under a Creative Commons Attribution 4.0 International License, which permits use, sharing, adaptation, distribution and reproduction in any medium or format, as long as you give appropriate credit to the original author(s) and the source, provide a link to the Creative Commons licence, and indicate if changes were made. The images or other third party material in this article are included in the article's Creative Commons licence, unless indicated otherwise in a credit line to the material. If material is not included in the article's Creative Commons licence and your intended use is not permitted by statutory regulation or exceeds the permitted use, you will need to obtain permission directly from the copyright holder. To view a copy of this licence, visit <http://creativecommons.org/licenses/by/4.0/>.

© The Author(s) 2024

Methods

Animals and study design

All experimental procedures were approved by the Animal Experiments Inspectorate under the Danish Ministry of Veterinary and Food Administration (protocol number 2016-15-0201-00884). Ten Danish Landrace pigs were included (48–52 kg, all of which were female). Female subjects were preferred due to their underrepresentation in existing literature^{40,41}, despite the fact that the majority of patients with chronic pain are female^{42,43}. Animals were acclimatized to the stable for 2 weeks before the experiment. Six animals underwent the NI model, and four control animals were subjected to sham intervention, as a greater heterogeneity was expected in NI compared with the control data. Technicians who were blinded to experimental groups randomly selected animals. Intervention and sham experiments were carried out interspersed so that any effect of surgical training would not influence the data in either experimental group. The cortical laminae in which the electrodes were placed were identified for seven animals (five intervention and two control). As this is one of the first studies investigating cortical changes in a porcine nerve damage model, the sample size was estimated based on typical group sizes in rodent studies of the same kind^{14,17,26} and pig studies involving NI^{24,31}.

Anesthesia

The animals were premedicated with an intramuscular injection of Zoletil Vet (1 ml per 10 kg; ketamine, 6.25 mg/ml; tiletamine, 6.25 mg/ml; zolazepam, 6.25 mg/ml; butorphanol, 1.25 mg/ml; and xylazine 6.5 mg/ml). The pigs were placed in a supine position and intubated. The jugular vein was cannulated for saline (0.9% NaCl) infusion. Anesthesia was maintained by infusion (6–10 ml/h) of propofol (10 mg/ml) and fentanyl (50 µg/ml) and ventilation with 1.5–3.0% sevoflurane. Blood pressure, heart rate, blood oxygenation, end-tidal CO₂ and temperature were continuously monitored, and anesthetic parameters were adjusted when needed⁴⁴. Temperature was maintained at 38 °C (±1 °C) by a forced air flow blanket placed over the animal (Mistral-Air Plus, MA1100-EU).

Peripheral surgery

Access to the peripheral nerves in the left forelimb was achieved through an incision in the axilla and blunt dissection of the superficial pectoralis muscle. The median and ulnar nerves were separated from connective tissue before placing bipolar cuff electrodes. Additionally, a cuff electrode was implanted on each nerve branch to record nerve responses with four bipolar channels. All cuffs were insulated using additional silicone sheets and secured using ligatures. Core temperature was kept stable and local temperature was monitored using a thermocouple probe secured to a nearby muscle, as sensory nerve recruitment and conduction are dependent on temperature⁴⁵.

A second incision was made on the lower anterior forelimb to expose the ulnar nerve. Two ligatures were loosely tied around the ulnar nerve as preparation for NI in intervention and control animals. After baseline recordings, the sutures were tied, and the nerve was cut between the sutures in the six intervention animals. The skin was closed with surgical staples during electrophysiological recordings.

Cranial surgery

The animal was placed in a prone position, and the head was placed in a custom-built localizer box and stereotaxic frame⁴⁶. This method allows high-precision insertion of the intracortical electrodes and prevents movement of the intracortical electrodes during other procedures. The skin was incised and retracted, and the periosteum was removed. A 5 × 5 cm² square craniectomy was performed to expose the contralateral S1 region using a Dremel (8228, Dremel) with a burr drill and rongeurs. The hole extended 1 cm ipsilateral to the sagittal and posterior to the coronal suture lines (see also ref. 34). Bone screws were placed lateral and anterior to the square to act as ground and reference for the intracortical recordings. A durotomy was initiated using a 23G bent needle to pierce the dura. The dura was further removed using precision forceps and sharp micro

scissors to expose S1. S1 was identified based on descriptions of Craner and Ray⁴⁷ and Sauleau et al.²²; the foundational model development is described elsewhere (W. Jensen, A. Hayward and C. R. Bjarkam, unpublished data). An electrode array with two shanks with eight channels each (E16-285-S2-L8-1100; ATLAS Neuroengineering) was lowered 3 mm into the brain using a manually driven micromanipulator. After 5 min to allow the brain tissue to adjust, the electrode was retracted so that the tip was at a depth of 1.5 mm. Electrophysiological recordings were conducted in anesthetized animals 40 min after electrode placement to allow the electrodes to settle in the tissue. The experimental timeline is shown in Supplementary Fig. 1.

Electrophysiology

Bipolar electrical stimulation was applied with a 3 mA cathodic-first pulse of 100 µs duration and an anodic phase of 375 µA and 800 µs duration, separated by a 100 µs interpulse interval. Stimulation was repeated 200 times at 2 Hz, alternating between the ulnar and median nerve, with random interstimulus interval to avoid adaptation. Stimulation series were performed at 10 min intervals. A total of 3 stimulation series were recorded before intervention and 18 after. Cortical data were recorded through an RX5 Pentusa Base Station system (Tucker-Davis Technologies) at 25 kHz, then high pass filtered at 300 Hz. A manual threshold (threshold equal to three to five times the RMS value of the background noise level) was used for online spike detection.

Histology

To determine in which layer the channels were located, histological analysis was performed for seven of the animals. A block around the electrode region of seven animals was cut and post-fixed in formalin (10% w/v) for 12 weeks. The tissue was then divided into 0.5 cm blocks, which were embedded in paraffin and sliced on a vibratome (10 µm thickness). Sections were Nissl stained using cresyl violet and slides were visualized by a slide scanner. NanoZoomer Digital Pathology View (version 2.2.1, Hamamatsu Photonics) was used for precise localization of the electrode contacts and identification of cortical layers²⁸. Contact sites were marked by electrochemically damaging the tissue surrounding the contacts using prolonged 1 mA monophasic electrical stimulation.

Data analysis

All spikes above the threshold were saved and used to construct PSTHs, using the spikes detected 50 ms before the peripheral stimulus and up to 450 ms after. All spikes detected after a single stimulus were divided into 1 ms bins and added together for each stimulation session consisting of 100 stimuli per nerve. The background activity was subtracted by removing the average spike count 50 ms to 5 ms before stimulus onset, to account for differences in thresholding.

Two peaks were visually distinguished in the PSTH, 10–20 ms after the stimulus and between 20 and 35 ms after the stimulus. PSTHs were, therefore, divided into two time windows: 10–19 ms and 21–35 ms after the stimulus. The peak amplitude was calculated as the maximum spike count within these time windows. The latency was calculated using the CoM for both time ranges, as follows:

$$\text{CoM} = \frac{1}{\sum_{t_1}^{t_2} \text{spikes}} \sum_{t_1}^{t_2} (\text{spikes} \times t),$$

where t_1 and t_2 are the lower and higher end of the time windows, 'spikes' is the spike count per bin and t is time.

Spikes recorded on all channels were averaged to investigate the effect of stimulation of the uninjured median and injured ulnar nerve on PSTH peak amplitude and latency. This is common practice for signals from the same brain area^{14,26}. The data were divided into 30 min phases consisting of three stimulation sessions, one phase before and six phases after the intervention. PSTH of the three sessions in a phase were averaged, after which peak amplitude and CoM were extracted.

For the analysis of the different layers, the responses to stimulation of the median and ulnar nerves were averaged, as there was no significant difference between them.

Channels that did not record a response to stimulation during any stimulation session throughout the experiment were removed. Eleven unresponsive channels were removed. Eight channels were from a single control experiment, where one shank was either misplaced or damaged. Two channels were located in layer I in a control animal and one channel was located in layer I in a NI experiment. To analyze whether responses differed per cortical layer, data from seven animals were used for which histology was performed. The number of channels per layer is presented in Table 1.

Spike sorting was performed in an automated manner using a custom-made analysis code. Principle component analysis was performed to identify the most relevant seven features: number of zero-crossings, peak width of the most prominent peak, amplitude and latency of the positive and negative peaks and whether the positive or negative polarity occurred first. The features that explained more than 10% of the variability were used in a *k*-means clustering algorithm. Few neurons per channel were expected, so the maximum number of clusters was set to five. The optimal number of clusters was identified using the silhouette method, which compares the similarity of the data within a cluster to the similarity between different clusters. Finally, the data were clustered into the optimal number of clusters identified by the silhouette method using *k*-means clustering.

Statistical analysis

To determine whether there was a difference in excitability when stimulating the injured compared with the uninjured nerve, three-way repeated measures ANOVA was used. Dependent variables were CoM and peak amplitude. Between-subject factors were control and NI; within-subject factors were time (one measurement before and six after intervention) and (uninjured) median and (injured) ulnar nerve. The stimulation of the two different nerves was assumed to activate two distinct populations of neurons in S1. From the ten datasets collected, one dataset was excluded due to missing data, resulting in six intervention and three control datasets. Normality of the data was verified using the Shapiro–Wilk test and the Q–Q plots.

Since the brain response from different layers after the same stimulus violates the independence assumption, a mixed model was used for the statistical analysis of the seven datasets for which histological analysis was performed. Fixed factors in the mixed model were layer, intervention and time. Time was also a repeated effect, which was modeled using a first-order autoregressive covariance matrix to account for the dependence of the data. Both slope and intercept were added as a random factor, which improved the quality of the model. A backwards approach was used to find the appropriate model, where the least significant fixed factors were removed sequentially until only significant factors remained. The resulting models are provided in Table 2.

For all models with significant interactions and significant main effects, pairwise comparisons were performed. These comparisons were used to answer three questions for each of the dependent variables (peak amplitude and CoM of the early and late peak):

- Does the evoked response to electrical stimulation differ between cortical layers?
- Is there a difference in cortical responses between the NI intervention and control group within each cortical layer and phase?
- Does the response within each layer differ after the NI intervention compared with the baseline?

The statistical tests were performed using SPSS version 27. Multiple comparisons were adjusted using the Bonferroni correction. The differences were considered statistically significant when $P < 0.05$. The estimated marginal means and standard error of the mean are reported.

Reporting summary

Further information on research design is available in the Nature Portfolio Reporting Summary linked to this article.

Data availability

The data that support the findings of this study are available from the corresponding author upon request.

References

40. Mogil, J. S. & Chanda, M. L. The case for the inclusion of female subjects in basic science studies of pain. *Pain* **117**, 1–5 (2005).
41. Mogil, J. S. Qualitative sex differences in pain processing: emerging evidence of a biased literature. *Nat. Rev. Neurosci.* **21**, 353–365 (2020).
42. Ruau, D., Liu, L. Y., Clark, J. D., Angst, M. S. & Butte, A. J. Sex differences in reported pain across 11,000 patients captured in electronic medical records. *J. Pain* **13**, 228–234 (2012).
43. Breivik, H., Eisenberg, E. & O'Brien, T. The individual and societal burden of chronic pain in Europe: the case for strategic prioritisation and action to improve knowledge and availability of appropriate care. *BMC Public Health* **13**, 1229 (2013).
44. Swindle, M. M. & Smith, A. C. (eds) *Swine in the Laboratory: Surgery, Anesthesia, Imaging, and Experimental Techniques* (Taylor and Francis Group, 2016).
45. Morris, J. Technical tips: methods of warming and maintaining limb temperature during nerve conduction studies. *Neurodiagn. J.* **53**, 241–251 (2013).
46. Bjarkam, C. R. et al. A MRI-compatible stereotaxic localizer box enables high-precision stereotaxic procedures in pigs. *J. Neurosci. Methods* **139**, 293–298 (2004).
47. Craner, S. L. & Ray, R. H. Somatosensory cortex of the neonatal pig: I. Topographic organization of the primary somatosensory cortex (SI). *J. Comp. Neurol.* **306**, 24–38 (1991).

Acknowledgements

This work was funded by the Center for Neuroplasticity and Pain. The Center for Neuroplasticity and Pain is supported by the Danish National Research Foundation (DNRF121). We thank the staff at the animal facilities for assistance during the experiments.

Author contributions

S.M. analyzed the data and drafted and revised the manuscript. A.J.H. and T.G.N.D.S.N. collected the data and reviewed the manuscript. C.R.B. designed the surgical methodology of the study, analyzed the histological data together with A.J.H. and reviewed the manuscript. W.J. conceptualized the study, supported data collection and analysis and reviewed the manuscript.

Funding

Open access funding provided by Aalborg University.

Competing interests

The authors declare no competing interests.

Additional information

Supplementary information The online version contains supplementary material available at <https://doi.org/10.1038/s41684-024-01440-0>.

Correspondence and requests for materials should be addressed to Suzan Meijs.

Peer review information *Lab Animal* thanks David Mor, Shiqian Shen and Hanns Zeilhofer for their contribution to the peer review of this work.

Reprints and permissions information is available at www.nature.com/reprints.

Reporting Summary

Nature Portfolio wishes to improve the reproducibility of the work that we publish. This form provides structure for consistency and transparency in reporting. For further information on Nature Portfolio policies, see our [Editorial Policies](#) and the [Editorial Policy Checklist](#).

Statistics

For all statistical analyses, confirm that the following items are present in the figure legend, table legend, main text, or Methods section.

n/a Confirmed

- The exact sample size (n) for each experimental group/condition, given as a discrete number and unit of measurement
- A statement on whether measurements were taken from distinct samples or whether the same sample was measured repeatedly
- The statistical test(s) used AND whether they are one- or two-sided
Only common tests should be described solely by name; describe more complex techniques in the Methods section.
- A description of all covariates tested
- A description of any assumptions or corrections, such as tests of normality and adjustment for multiple comparisons
- A full description of the statistical parameters including central tendency (e.g. means) or other basic estimates (e.g. regression coefficient) AND variation (e.g. standard deviation) or associated estimates of uncertainty (e.g. confidence intervals)
- For null hypothesis testing, the test statistic (e.g. F , t , r) with confidence intervals, effect sizes, degrees of freedom and P value noted
Give P values as exact values whenever suitable.
- For Bayesian analysis, information on the choice of priors and Markov chain Monte Carlo settings
- For hierarchical and complex designs, identification of the appropriate level for tests and full reporting of outcomes
- Estimates of effect sizes (e.g. Cohen's d , Pearson's r), indicating how they were calculated

Our web collection on [statistics for biologists](#) contains articles on many of the points above.

Software and code

Policy information about [availability of computer code](#)

Data collection TDT's Synapse was used.

Data analysis Data was analyzed using custom code in matlab, using a typical data analysis paradigm.

For manuscripts utilizing custom algorithms or software that are central to the research but not yet described in published literature, software must be made available to editors and reviewers. We strongly encourage code deposition in a community repository (e.g. GitHub). See the Nature Portfolio [guidelines for submitting code & software](#) for further information.

Data

Policy information about [availability of data](#)

All manuscripts must include a [data availability statement](#). This statement should provide the following information, where applicable:

- Accession codes, unique identifiers, or web links for publicly available datasets
- A description of any restrictions on data availability
- For clinical datasets or third party data, please ensure that the statement adheres to our [policy](#)

Data is available upon request.

Field-specific reporting

Please select the one below that is the best fit for your research. If you are not sure, read the appropriate sections before making your selection.

Life sciences Behavioural & social sciences Ecological, evolutionary & environmental sciences

For a reference copy of the document with all sections, see [nature.com/documents/nr-reporting-summary-flat.pdf](https://www.nature.com/documents/nr-reporting-summary-flat.pdf)

Life sciences study design

All studies must disclose on these points even when the disclosure is negative.

Sample size 10 animals, brain histology was performed for 7 of these.

Data exclusions One dataset was excluded due to missing data.

Replication The experiment was repeated in the 10 animals, yielding consistent results analyzed with statistical methods as described in the manuscript.

Randomization Random selection of animals on the day of the experiment.

Blinding Technicians selecting the animals were blinded to group allocation.

Reporting for specific materials, systems and methods

We require information from authors about some types of materials, experimental systems and methods used in many studies. Here, indicate whether each material, system or method listed is relevant to your study. If you are not sure if a list item applies to your research, read the appropriate section before selecting a response.

Materials & experimental systems

n/a | Involved in the study

Antibodies

Eukaryotic cell lines

Palaeontology and archaeology

Animals and other organisms

Human research participants

Clinical data

Dual use research of concern

Methods

n/a | Involved in the study

ChIP-seq

Flow cytometry

MRI-based neuroimaging

Antibodies

Antibodies used Describe all antibodies used in the study; as applicable, provide supplier name, catalog number, clone name, and lot number.

Validation Describe the validation of each primary antibody for the species and application, noting any validation statements on the manufacturer's website, relevant citations, antibody profiles in online databases, or data provided in the manuscript.

Eukaryotic cell lines

Policy information about [cell lines](#)

Cell line source(s) State the source of each cell line used.

Authentication Describe the authentication procedures for each cell line used OR declare that none of the cell lines used were authenticated.

Mycoplasma contamination Confirm that all cell lines tested negative for mycoplasma contamination OR describe the results of the testing for mycoplasma contamination OR declare that the cell lines were not tested for mycoplasma contamination.

Commonly misidentified lines (See [ICLAC](#) register) Name any commonly misidentified cell lines used in the study and provide a rationale for their use.

Palaeontology and Archaeology

Specimen provenance Provide provenance information for specimens and describe permits that were obtained for the work (including the name of the

Specimen provenance

Specimen deposition

Dating methods

Tick this box to confirm that the raw and calibrated dates are available in the paper or in Supplementary Information.

Ethics oversight

Note that full information on the approval of the study protocol must also be provided in the manuscript.

Animals and other organisms

Policy information about [studies involving animals](#); [ARRIVE guidelines](#) recommended for reporting animal research

Laboratory animals

Wild animals

Field-collected samples

Ethics oversight

Note that full information on the approval of the study protocol must also be provided in the manuscript.

Human research participants

Policy information about [studies involving human research participants](#)

Population characteristics

Recruitment

Ethics oversight

Note that full information on the approval of the study protocol must also be provided in the manuscript.

Clinical data

Policy information about [clinical studies](#)

All manuscripts should comply with the ICMJE [guidelines for publication of clinical research](#) and a completed [CONSORT checklist](#) must be included with all submissions.

Clinical trial registration

Study protocol

Data collection

Outcomes

Dual use research of concern

Policy information about [dual use research of concern](#)

Hazards

Could the accidental, deliberate or reckless misuse of agents or technologies generated in the work, or the application of information presented in the manuscript, pose a threat to:

No	Yes
<input checked="" type="checkbox"/>	<input type="checkbox"/> Public health
<input checked="" type="checkbox"/>	<input type="checkbox"/> National security
<input checked="" type="checkbox"/>	<input type="checkbox"/> Crops and/or livestock
<input checked="" type="checkbox"/>	<input type="checkbox"/> Ecosystems
<input checked="" type="checkbox"/>	<input type="checkbox"/> Any other significant area

Experiments of concern

Does the work involve any of these experiments of concern:

No	Yes
<input checked="" type="checkbox"/>	<input type="checkbox"/> Demonstrate how to render a vaccine ineffective
<input checked="" type="checkbox"/>	<input type="checkbox"/> Confer resistance to therapeutically useful antibiotics or antiviral agents
<input checked="" type="checkbox"/>	<input type="checkbox"/> Enhance the virulence of a pathogen or render a nonpathogen virulent
<input checked="" type="checkbox"/>	<input type="checkbox"/> Increase transmissibility of a pathogen
<input checked="" type="checkbox"/>	<input type="checkbox"/> Alter the host range of a pathogen
<input checked="" type="checkbox"/>	<input type="checkbox"/> Enable evasion of diagnostic/detection modalities
<input checked="" type="checkbox"/>	<input type="checkbox"/> Enable the weaponization of a biological agent or toxin
<input checked="" type="checkbox"/>	<input type="checkbox"/> Any other potentially harmful combination of experiments and agents

ChIP-seq

Data deposition

- Confirm that both raw and final processed data have been deposited in a public database such as [GEO](#).
- Confirm that you have deposited or provided access to graph files (e.g. BED files) for the called peaks.

Data access links

May remain private before publication.

For "Initial submission" or "Revised version" documents, provide reviewer access links. For your "Final submission" document, provide a link to the deposited data.

Files in database submission

Provide a list of all files available in the database submission.

Genome browser session

(e.g. [UCSC](#))

Provide a link to an anonymized genome browser session for "Initial submission" and "Revised version" documents only, to enable peer review. Write "no longer applicable" for "Final submission" documents.

Methodology

Replicates

Describe the experimental replicates, specifying number, type and replicate agreement.

Sequencing depth

Describe the sequencing depth for each experiment, providing the total number of reads, uniquely mapped reads, length of reads and whether they were paired- or single-end.

Antibodies

Describe the antibodies used for the ChIP-seq experiments; as applicable, provide supplier name, catalog number, clone name, and lot number.

Peak calling parameters

Specify the command line program and parameters used for read mapping and peak calling, including the ChIP, control and index files used.

Data quality

Describe the methods used to ensure data quality in full detail, including how many peaks are at FDR 5% and above 5-fold enrichment.

Software

Describe the software used to collect and analyze the ChIP-seq data. For custom code that has been deposited into a community repository, provide accession details.

Flow Cytometry

Plots

Confirm that:

- The axis labels state the marker and fluorochrome used (e.g. CD4-FITC).
- The axis scales are clearly visible. Include numbers along axes only for bottom left plot of group (a 'group' is an analysis of identical markers).
- All plots are contour plots with outliers or pseudocolor plots.
- A numerical value for number of cells or percentage (with statistics) is provided.

Methodology

Sample preparation

Describe the sample preparation, detailing the biological source of the cells and any tissue processing steps used.

Instrument

Identify the instrument used for data collection, specifying make and model number.

Software

Describe the software used to collect and analyze the flow cytometry data. For custom code that has been deposited into a community repository, provide accession details.

Cell population abundance

Describe the abundance of the relevant cell populations within post-sort fractions, providing details on the purity of the samples and how it was determined.

Gating strategy

Describe the gating strategy used for all relevant experiments, specifying the preliminary FSC/SSC gates of the starting cell population, indicating where boundaries between "positive" and "negative" staining cell populations are defined.

- Tick this box to confirm that a figure exemplifying the gating strategy is provided in the Supplementary Information.

Magnetic resonance imaging

Experimental design

Design type

Indicate task or resting state; event-related or block design.

Design specifications

Specify the number of blocks, trials or experimental units per session and/or subject, and specify the length of each trial or block (if trials are blocked) and interval between trials.

Behavioral performance measures

State number and/or type of variables recorded (e.g. correct button press, response time) and what statistics were used to establish that the subjects were performing the task as expected (e.g. mean, range, and/or standard deviation across subjects).

Acquisition

Imaging type(s)

Specify: functional, structural, diffusion, perfusion.

Field strength

Specify in Tesla

Sequence & imaging parameters

Specify the pulse sequence type (gradient echo, spin echo, etc.), imaging type (EPI, spiral, etc.), field of view, matrix size, slice thickness, orientation and TE/TR/flip angle.

Area of acquisition

State whether a whole brain scan was used OR define the area of acquisition, describing how the region was determined.

Diffusion MRI

Used

Not used

Preprocessing

Preprocessing software

Provide detail on software version and revision number and on specific parameters (model/functions, brain extraction, segmentation, smoothing kernel size, etc.).

Normalization

If data were normalized/standardized, describe the approach(es): specify linear or non-linear and define image types used for transformation OR indicate that data were not normalized and explain rationale for lack of normalization.

Normalization template

Describe the template used for normalization/transformation, specifying subject space or group standardized space (e.g. original Talairach, MNI305, ICBM152) OR indicate that the data were not normalized.

Noise and artifact removal

Describe your procedure(s) for artifact and structured noise removal, specifying motion parameters, tissue signals and physiological signals (heart rate, respiration).

Volume censoring

Define your software and/or method and criteria for volume censoring, and state the extent of such censoring.

Statistical modeling & inference

Model type and settings

Specify type (mass univariate, multivariate, RSA, predictive, etc.) and describe essential details of the model at the first and second levels (e.g. fixed, random or mixed effects; drift or auto-correlation).

Effect(s) tested

Define precise effect in terms of the task or stimulus conditions instead of psychological concepts and indicate whether ANOVA or factorial designs were used.

Specify type of analysis: Whole brain ROI-based BothStatistic type for inference
(See [Eklund et al. 2016](#))

Specify voxel-wise or cluster-wise and report all relevant parameters for cluster-wise methods.

Correction

Describe the type of correction and how it is obtained for multiple comparisons (e.g. FWE, FDR, permutation or Monte Carlo).

Models & analysis

n/a | Involved in the study

 Functional and/or effective connectivity Graph analysis Multivariate modeling or predictive analysis

Functional and/or effective connectivity

Report the measures of dependence used and the model details (e.g. Pearson correlation, partial correlation, mutual information).

Graph analysis

Report the dependent variable and connectivity measure, specifying weighted graph or binarized graph, subject- or group-level, and the global and/or node summaries used (e.g. clustering coefficient, efficiency, etc.).

Multivariate modeling and predictive analysis

Specify independent variables, features extraction and dimension reduction, model, training and evaluation metrics.